Astron. Astrophys. 358, 682–688 (2000)

ASTRONOMY AND ASTROPHYSICS

Low-J CO line emission from PDRs: a natural explanation for the narrow range of observed line ratios

H. Störzer[1], **M. Zielinsky**[1], **J. Stutzki**[1], **and A. Sternberg**[2]

[1] I. Physikalisches Institut der Universität zu Köln, Zülpicher Strasse 77, 50937 Köln, Germany
[2] Tel Aviv University, School of Physics and Astronomy, Ramat Aviv, Israel

Received 10 August 1999/ Accepted 18 February 2000

Abstract. We argue that the surprisingly narrow range of low-J ^{12}CO, ^{13}CO and C^{18}O line ratios observed in massive star-formation regions is naturally explained if the CO emission is understood to arise in an ensemble of dense clumps which are embedded in a lower-density interclump medium which is pervaded by stellar radiation. We demonstrate this by presenting PDR computations which focus explicitly on the ^{12}CO, ^{13}CO and C^{18}O $J = 1 \rightarrow 0$, $J = 2 \rightarrow 1$ and $J = 3 \rightarrow 2$ rotational line emission for a wide range of cloud conditions. We consider spherical clouds which are illuminated by isotropic far-ultraviolet (FUV) radiation fields. Our models provide a self-consistent treatment of the chemical and thermal balance together with the radiative transfer of the CO line emission. We present results for clouds with power-law density gradients with average hydrogen particle densities $\langle n \rangle$ ranging from 10^4 to $10^7 \mathrm{cm}^{-3}$ and total average hydrogen column densities $\langle N \rangle$ between 2.5×10^{21} and $4.0 \times 10^{22} \mathrm{cm}^{-2}$. We consider clouds exposed to FUV fields (χ) 10^2 to 10^4 times more intense than the mean interstellar radiation field. We find that the resulting line ratios are insensitive to the cloud conditions and reproduce the observed values of the relative CO line strengths.

Key words: radiative transfer – ISM: clouds – ISM: molecules – ISM: structure

1. Introduction

Observations of low-J ^{12}CO and ^{13}CO $J = 1 \rightarrow 0$, $J = 2 \rightarrow 1$ and $J = 3 \rightarrow 2$ emission lines in several star-forming molecular cloud complexes (Castets et al. 1990; Sakamoto et al. 1994; Röhrig et al. 1995; Kramer et al. 1996; Schneider et al. 1998; Wilson et al. 1999) show that the measured line intensities and ratios cannot be produced in clouds of uniform gas temperature and density.

Typically the $J = 2 \rightarrow 1/J = 1 \rightarrow 0$ intensity ratios for both ^{12}CO and ^{13}CO are close to unity. This appears to indicate optically thick thermalized emission in a homogeneous cloud for two reasons. First, if the emission were optically thin then the line ratios would be significantly greater than ~ 1 because of the smaller optical depth of the $1 \rightarrow 0$ transitions. Second, if the total hydrogen density in the emitting regions were smaller than the critical density required to thermalize the populations in the $J = 2$ levels then the line ratios would become smaller than 1 due to the smaller critical densities required for thermalization of the $J = 1$ levels. However, the isotopic ^{12}CO/^{13}CO ratio of $J = 2 \rightarrow 1$ and $J = 1 \rightarrow 0$ ranges from 2 to 8. For homogeneous media this indicates optically *thin* rather than optically thick ^{13}CO emission. Thus, the various CO emission lines cannot be produced in homogeneous media of uniform temperature and density. Similar results have been found in several starburst galaxies (Aalto et al. 1995; Papadopoulos & Seaquist 1998) where the isotopic ^{12}CO/^{13}CO ratios are even larger (~ 13). Castets et al. (1990) noted that external heating with the corresponding inside-out temperature gradient can explain the observed line ratios. However, as we discuss below, the relatively narrow range of observed line ratios, as discussed below, however, requires a relatively universal astrophysical scenario for this external heating.

Observations of C$^+$ and C^{18}O in these star-forming regions have shown (cf. Stutzki et al. 1988; van der Werf et al. 1995) that the clouds are not homogeneous, but are in fact clumpy and consist of at least two components with high density contrast. In a clumpy environment the higher density condensations, or clumps, are illuminated by stellar FUV radiation which penetrates and is scattered through the lower-density interclump medium. Dense photon dominated regions (PDRs) (cf. Sternberg & Dalgarno 1995) form on the surfaces of the clumps. In such clumps the gas temperature decreases from the FUV heated surface layers to the colder shielded cores. As discussed in detail by Störzer et al. (1996), because of the temperature gradients, as well as geometrical effects (e.g. clumps will appear smaller in optically thinner ^{13}CO lines compared to optically thicker ^{12}CO lines) both the absolute and relative intensities of ^{12}CO, ^{13}CO and C^{18}O emission lines will differ considerably from those produced in homogeneous clouds and plane parallel geometries.

Recent studies have shown that the observed complex structure of the molecular cloud emission can be well fitted by a decomposition of the cloud into many clumps. Typically, the clumps identified follow a power law mass distribution and mass–size relation (Kramer et al. 1998; Heithausen et al. 1998). Alternatively, the structure can be characterized as frac-

Send offprint requests to: J. Stutzki (stutzki@ph1.uni-koeln.de)

tal. Stutzki et al. (1998) recently demonstrated that these two, at first sight apparently conflicting scenarios are in fact consistent: an ensemble of clumps with the given mass and size spectrum results in a fractal structure of the cloud image. This background suggests that the combined emission of an ensemble of clumps, where each clump is modeled as a spherical cloud in an embedding UV field, can reproduce the observed line intensities. In this paper we show, that the low–J CO and isotopomeric CO line emission ratios of spherical clumps are indeed rather insensitive to the details of the clump parameters (density, column density; and hence size and mass) and the strength of the embedding UV field (and hence position in the cloud). Further, we show that the line ratios match the narrow range of observed values. This then implies that the emission properties of the entire ensemble will be almost identical to those of the single clumps we study in this paper.

Several efforts have been made to model the observed ^{12}CO/^{13}CO line intensities emitted by higher density molecular condensations, exposed to FUV radiation in clumpy environments. Gierens et al. (1992) performed carbon monoxide line radiative transfer computations for spherically symmetric, FUV illuminated molecular clumps. The model reproduces successfully the low-J CO line intensities observed in the Orion A molecular cloud. Köster et al. (1994) presented the ^{12}CO/^{13}CO line intensities for finite-sized, plane-parallel PDRs.

In this paper we present a set of calculations over a large parameter range for the ^{12}CO/^{13}CO/C^{18}O low-J line intensities emitted by spherical molecular clouds which are heated by an external FUV field. In contrast with the Gierens et al. models we do not use an analytical approximation for the temperature structure, and the CO and H_2 density distribution, but we compute the PDR structure numerically and use the numerical results as input for the radiative transfer program of Gierens et al. This procedure provides the most realistic computation to-date of the low-J ^{12}CO, ^{13}CO and C^{18}O emission line intensities which depend sensitively on both the CO density structures (for each isotope) and temperature distributions in the clouds. Unlike the plane-parallel models by Köster et al. we assume spherical geometry for the clouds (Störzer et al. 1996; see also Spaans & Neufeld 1997). As in Störzer et al. we consider clouds with gas densities which increase toward the cloud centers. In Sect. 2 we describe the basics of our model, in Sect. 3 we discuss the resulting ^{12}CO/^{13}CO/C^{18}O low-J line intensities for a range of assumed hydrogen gas densities, column densities (i.e. cloud sizes), and FUV field intensities. In Sect. 4 we compare our results with observations, and summarize our results in Sect. 5.

2. Spherical PDR models

Our method for calculating the chemical and physical structure of the spherical PDRs is described in detail in Störzer et al. (1996). The basic assumptions of our models are as follows. First, the clouds are assumed to be spherically symmetric. Second, the clouds are exposed to isotropic FUV fields. Third, the total hydrogen particle density $n(r)$ increases radially inward and is described by a power law of the form $n(r) = n_0(r/R)^{-1.5}$, where n_0 is the density at the clump surface and R is the total clump radius.

The main parameters of the models are: the volume average hydrogen particle density $\langle n \rangle$, the average projected hydrogen particle column density $\langle N \rangle$ and the intensity of the FUV field χ relative to the mean interstellar UV field (Draine 1978). The models presented here differ in three ways from the models presented in Störzer et al. (1996). First, we use the photoelectric heating rates of Bakes & Tielens (1994). The Bakes & Tielens (1994) photoelectric heating rates are larger in the CO emitting regions than the previously used rates of Draine (1978), resulting in somewhat stronger CO line intensities.

Second, we have included the ^{18}O chemistry. We assume a [^{12}C]/[^{13}C] abundance ratio of 67 and a [^{16}O]/[^{18}O] abundance ratio of 500. The chemical network includes the isotopic fractionation reactions listed by Langer et al. (1984). It is based on the most recent release of the UMIST network (Millar et al. 1997) with the relevant isotopically substituted C and O bearing species and corresponding reaction rates added, similar to what is described in Le Bourlot et al. (1993). We use an unattenuated CO photodissociation rate of $2.0 \times 10^{-10}\mathrm{s}^{-1}$ and employ the ^{12}CO/^{13}CO/C^{18}O self-shielding factors given by van Dishoeck & Black (1988).

Third, the dust temperature is calculated by using the formalism described in Hollenbach et al. (1991). This formalism takes into account that the dust inside the clouds is heated by a combination of the externally incident FUV radiation and, at large cloud depth, by the infrared (IR) continuum radiation emitted by warm dust in the FUV heated surface layers. Heating by IR radiation results in dust temperatures of 10 – 40 K in the cloud cores, depending on the strength of the incident FUV field. The warm dust in the FUV shielded cores is particularly important for the C^{18}O lines which are produced at large cloud depths.

As is discussed in Störzer et al. (1996), in our spherical PDR model we treat the line radiative transfer using an escape probability formalism when iteratively calculating the thermal structure as a balance between the gas heating and cooling. We use a more sophisticated multi-shell radiative transfer code to calculated the emergent line intensities after the final thermal and chemical structure of the spherical PDR is established. For those species considered in the heating and cooling balance, the differences between the line intensities that would be derived in the escape probability formalism and those calculated in the full radiative transfer are marginal.

In order to achieve a reasonably fast numerical treatment of each spherical PDR model, we had to keep the chemistry relatively simple. In particular, we did not including sulphur bearing species. Sulphur may affect the degree of ionization in the cloud, and has some effect on the location and temperature of the CI/CO transition layer (see e.g. Sternberg & Dalgarno 1995). Proper treatment of sulphur within the chemical network should thus be included in future applications of our spherical PDR model, but was beyond the scope of the present study.

In the following models we concentrate on FUV fields in the range $10^2 \leq \chi \leq 10^4$, which are typical values for many star

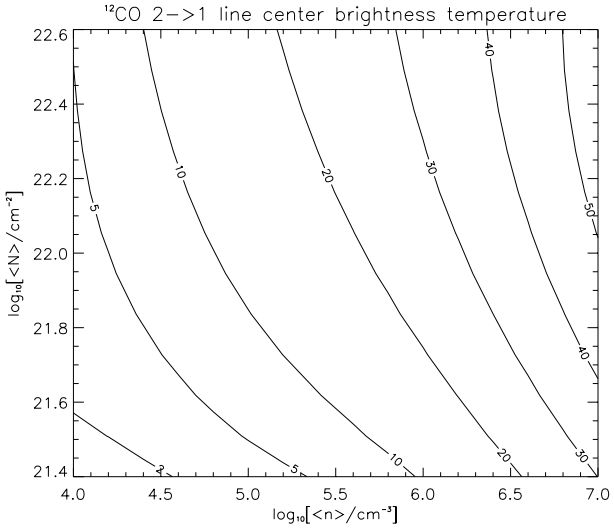

Fig. 1. Contours of the ^{12}CO 2→1 line center brightness temperature (in K) as a function of the volume average hydrogen particle density $\langle n\rangle$ and the average projected hydrogen particle column density $\langle N\rangle$ for $\chi = 10^3$.

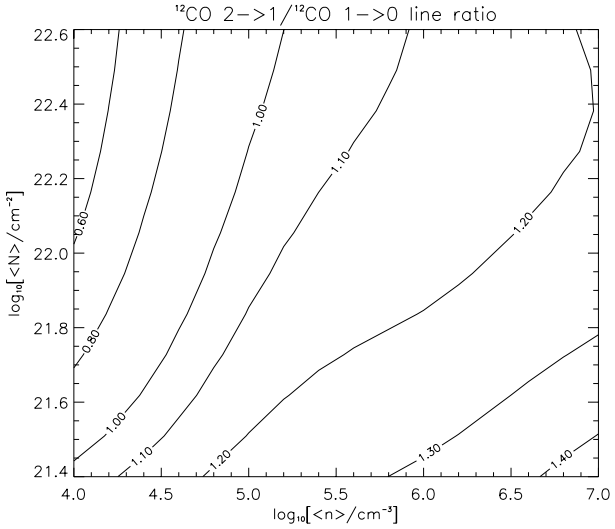

Fig. 2. Contours of the ^{12}CO 2→1/^{12}CO 1→0 line center brightness temperature ratio as a function of the volume average hydrogen particle density $\langle n\rangle$ and the average projected hydrogen particle column density $\langle N\rangle$ for $\chi = 10^3$.

Table 1. Model parameters

H fractional abundance	1.0
He fractional abundance	1.0×10^{-1}
O fractional abundance	5.0×10^{-4}
^{12}C fractional abundance	3.0×10^{-4}
Effective UV continuum absorption cross section	$\sigma_d = 1.9 \cdot 10^{-21}\mathrm{cm}^2$
Line width (FWHM)	b = 1.2 km sec^{-1}

forming cloud complexes, and vary the two other parameters between $10^4\mathrm{cm}^{-3} \le \langle n\rangle \le 10^7\mathrm{cm}^{-3}$ and $2.5 \times 10^{21}\mathrm{cm}^{-2} \le \langle N\rangle \le 4.0 \times 10^{22}\mathrm{cm}^{-2}$. This range of densities and column densities corresponds to cloud sizes of $R = 6.0 \times 10^{-5}$ pc to $R = 1.0$ pc. Other model parameters are listed in Table 1.

The ^{12}CO/^{13}CO/C^{18}O low-J line center brightness temperatures (see Köster et al. 1994 for a definition), i.e. the intensities of the $J = 1 \to 0$, $J = 2 \to 1$ and $J = 3 \to 2$ transitions, presented in the following section are given by the projected average of the intensity $\bar{I}$ over the clump surface (see Störzer et al. 1996). For large clouds $\langle N\rangle = 4.0 \cdot 10^{22}\mathrm{cm}^{-2}$, where the PDR is a thin surface shell, $\bar{I}$ corresponds very well to the intensity emitted by a plane-parallel, semi-infinite slab. However, for small clouds, where most of the carbon is in the form of C^+ and CO is only formed in the high density core, $\bar{I}$ can differ significantly from values produced in plane-parallel models. Limb-brightening effects have a less important effect on the emitted line intensities.

3. Line intensities

3.1. Fixed FUV field intensity

Fig. 1 displays contours of constant ^{12}CO 2→1 line center brightness temperatures, $\bar{I}$, as a function of the volume average hydrogen particle density $\langle n\rangle$ and the average projected hydrogen particle column density $\langle N\rangle$ for a fixed value of the FUV field intensity, $\chi = 10^3$. For fixed $\langle N\rangle$ the line intensity increases with $\langle n\rangle$ because the chemical formation of CO is more efficient for larger densities compared to the CO photodestruction. The CO emission region is, therefore, shifted in layers with higher temperatures. For small clouds, i.e. small values for $\langle N\rangle$, CO is present only in the clump cores, so that $\bar{I}$ decreases for fixed $\langle n\rangle$ and decreasing column densities $\langle N\rangle$. The ^{12}CO 2→1 line center brightness temperature varies from 1.1 K for a model with $\langle n\rangle = 10^4\mathrm{cm}^{-3}$ and $\langle N\rangle = 2.5 \cdot 10^{21}\mathrm{cm}^{-2}$ to 53 K for a model with $\langle n\rangle = 10^7\mathrm{cm}^{-3}$ and $\langle N\rangle = 4.0 \cdot 10^{22}\mathrm{cm}^{-2}$. The corresponding ^{13}CO 2→1 line intensities vary from 0.5 K to 24 K. C^{18}O is nearly fully dissociated in small clumps, and the C^{18}O 2→1 intensities reach maximum values of about 4 K in the limit of large $\langle n\rangle$ and $\langle N\rangle$.

Fig. 2 displays the ^{12}CO 2→1/^{12}CO 1→0 line center brightness temperature ratio in the $\langle n\rangle$ vs. $\langle N\rangle$ plane. This line ratio is insensitive to the density or cloud size. For large $\langle N\rangle$ and densities smaller than about $3 \cdot 10^4\mathrm{cm}^{-3}$ the line ratio is less than 1. At higher densities the ratio is slightly larger than 1. When the column density $\langle N\rangle$ is large the ^{12}CO lines are emitted from the surface layers of the spherical clumps where the gas densities are equal to about $n(r) = \langle n\rangle/2$. The critical density for collisional de-excitation of the 1→0 transition is $n_{\mathrm{cr}} \approx 3 \times 10^3\mathrm{cm}^{-3}$ and the $J = 1$ level population is always thermalized in our models. However, the critical density for the 2→1 transition is $n_{\mathrm{cr}} \approx 2 \cdot 10^4\mathrm{cm}^{-3}$ so that in our lower density models the $J = 2$ levels are subthermally excited. Therefore, the ^{12}CO 2→1/^{12}CO 1→0 line ratio is less than 1 in the low density, large column density models. At high densities the $J = 2$ level is thermalized as well, but because of the higher optical depth of the 2→1 transition it is emitted from warmer layers than the 1→0 line, and the ^{12}CO 2→1/^{12}CO 1→0 ratio is larger than

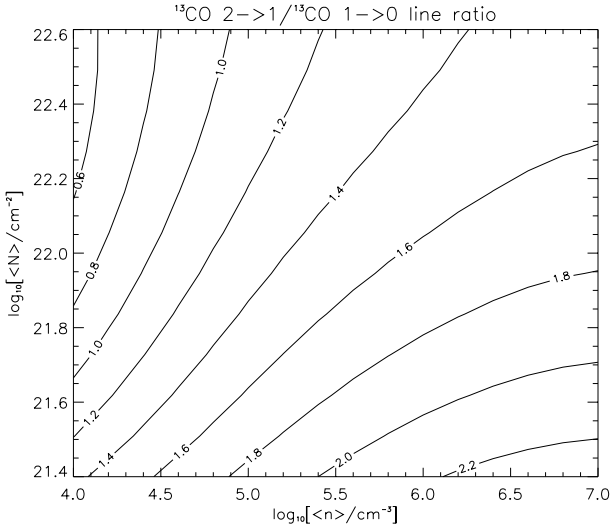

Fig. 3. Contours of the ^{13}CO 2→1/^{13}CO 1→0 line center brightness temperature ratio as a function of the volume average hydrogen particle density $\langle n\rangle$ and the average projected hydrogen particle column density $\langle N\rangle$ for $\chi = 10^3$.

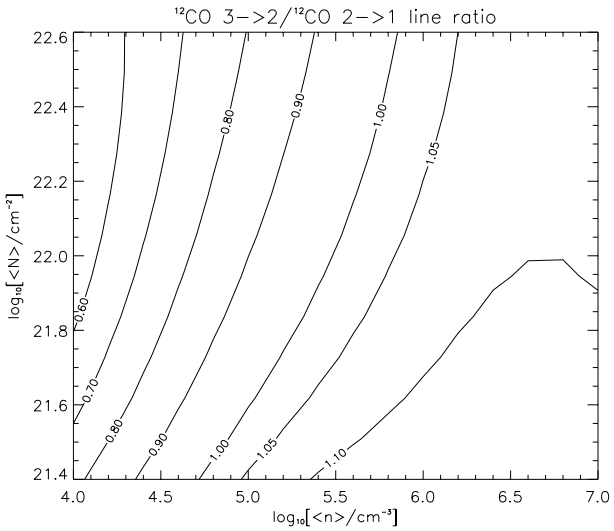

Fig. 4. Contours of the ^{12}CO 3→2/^{12}CO 2→1 line center brightness temperature ratio as a function of the volume average hydrogen particle density $\langle n\rangle$ and the average projected hydrogen particle column density $\langle N\rangle$ for $\chi = 10^3$.

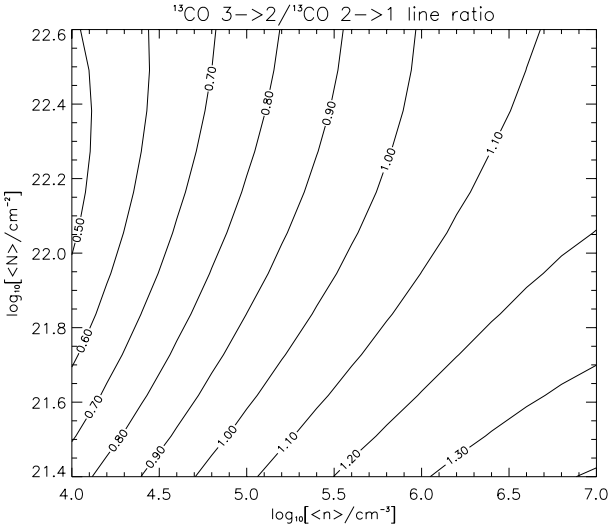

Fig. 5. Contours of the ^{13}CO 3→2/^{13}CO 2→1 line center brightness temperature ratio as a function of the volume average hydrogen particle density $\langle n\rangle$ and the average projected hydrogen particle column density $\langle N\rangle$ for $\chi = 10^3$.

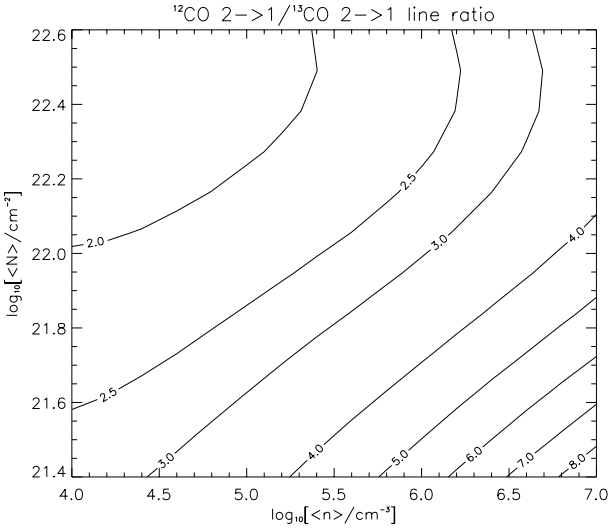

Fig. 6. Contours of the ^{12}CO 2→1/^{13}CO 2→1 line center brightness temperature ratio as a function of the volume average hydrogen particle density $\langle n\rangle$ and the average projected hydrogen particle column density $\langle N\rangle$ for $\chi = 10^3$.

1. When $\langle N\rangle$ and $\langle n\rangle$ are both small the CO lines are formed mainly in the cloud cores. Because of the density gradient the cores are denser than the surface layers and therefore the line ratio increases with $\langle N\rangle$ when $\langle n\rangle$ is small ($\lesssim 2 \cdot 10^4 \mathrm{cm}^{-3}$). For higher densities the 2→1/1→0 ratio decreases with $\langle N\rangle$ because limb-brightening becomes more important for smaller sized clouds.

Fig. 3 displays the ^{13}CO 2→1/^{13}CO 1→0 line ratio. The behavior is similar to the ^{12}CO 2→1/^{12}CO 1→0 ratio. For fixed $\langle n\rangle$ the ratio decreases for increasing $\langle N\rangle$, and for fixed $\langle N\rangle$ the ratio increases with $\langle n\rangle$. Because of the smaller optical depths of the ^{13}CO lines compared with the ^{12}CO lines the ^{13}CO line ratio attains somewhat larger values.

The ^{12}CO 3→2/2→1 and ^{13}CO 3→2/2→1 ratios displayed in Figs. 4 and 5 show a similar behavior. For gas densities less than the critical density ($\approx 7 \times 10^4 \mathrm{cm}^{-3}$) of the 3→2 transition the ratios are smaller than 1, and increase above unity at larger densities. However, the variation in the line ratio is even smaller than for the 2→1/1→0 ratios.

The isotopic ratio of the ^{12}CO and the ^{13}CO 2→1 lines is displayed in Fig. 6. The ratio ranges from 1.8 when $\langle n\rangle$ is small and $\langle N\rangle$ is large, to values of 8.0 when $\langle n\rangle$ is large and $\langle N\rangle$ is small. This ratio is sensitive to the temperature gradient.

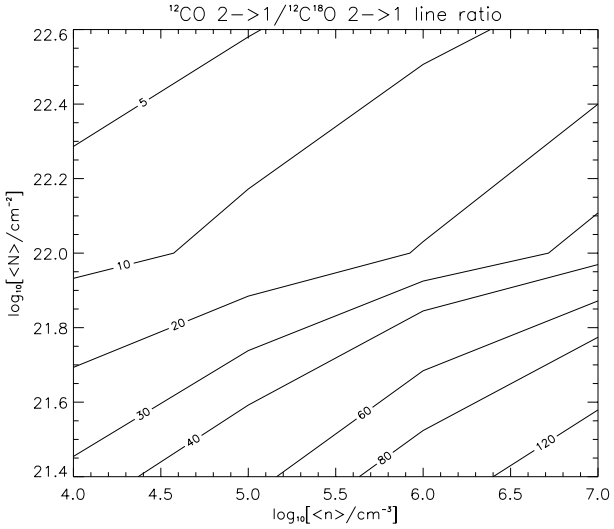

Fig. 7. Contours of the ^{12}CO 2→1/C^{18}O 2→1 line center brightness temperature ratio as a function of the volume average hydrogen particle density $\langle n\rangle$ and the average projected hydrogen particle column density $\langle N\rangle$ for $\chi = 10^3$.

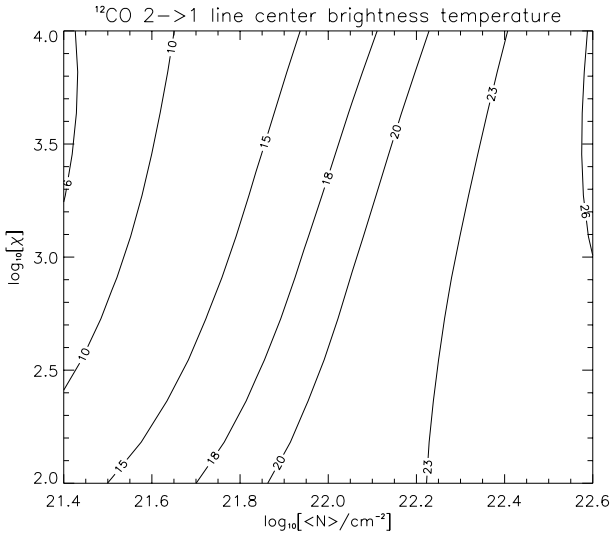

Fig. 8. Contours of the ^{12}CO 2→1 line center brightness temperature (in K) as a function of the average projected hydrogen particle column density $\langle N\rangle$ and the FUV field χ for a volume average hydrogen particle density $\langle n\rangle$=4 × 10^{5}cm^{-3}.

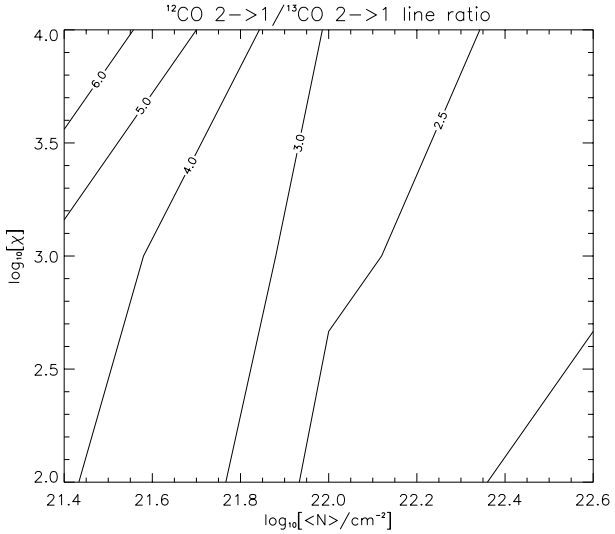

Fig. 9. Contours of the ^{12}CO 2→1/^{13}CO 2→1 line center brightness temperature ratio as a function of the average projected hydrogen particle column density $\langle N\rangle$ and the FUV field χ for a volume average hydrogen particle density $\langle n\rangle$=4 × 10^{5}cm^{-3}.

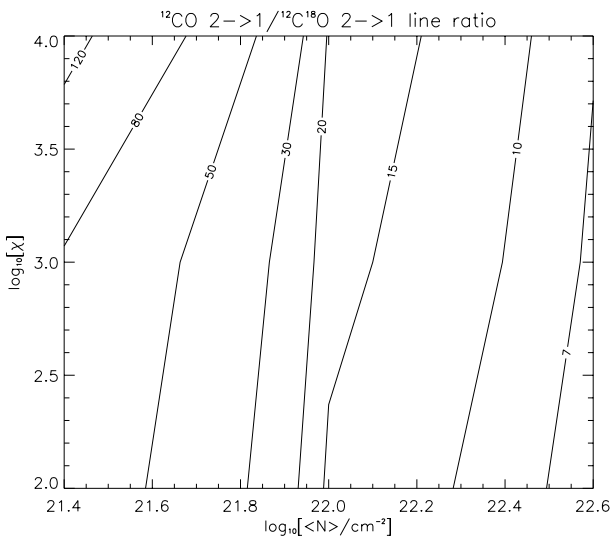

Fig. 10. Contours of the ^{12}CO 2→1/^{12}C^{18}O 2→1 line center brightness temperature ratio as a function of the average projected hydrogen particle column density $\langle N\rangle$ and the FUV field χ for a volume average hydrogen particle density $\langle n\rangle$=4 × 10^{5}cm^{-3}.

The ^{12}CO lines are formed in warm FUV heated surface layers, whereas the ^{13}CO lines are emitted from cooler regions closer to the cloud cores. This line ratio is also affected by the different optical depths of the ^{12}CO and the ^{13}CO 2→1 lines. This difference implies that the spherical clouds are effectively smaller for the ^{13}CO transitions than for the ^{12}CO transitions. The effect of the temperature gradient is most important for the high-density clouds, and the optical depth effect becomes significant for low $\langle N\rangle$ (i.e. small) clouds. The line ratio therefore increases as $\langle n\rangle$ increases and $\langle N\rangle$ decreases.

Fig. 7 shows the isotopic ratio of the ^{12}CO and the C^{18}O 2→1 line intensities. The behavior is similar to the ^{12}CO/^{13}CO ratio, but with larger values due to the much smaller C^{18}O abundances. The ^{12}CO/C^{18}O 2→1 ratio varies from 3 to > 100, reaching the large values at low column densities and high densities where the total amount of C^{18}O in the clump gets small enough that the C^{18}O lines actually become optically thin.

3.2. Fixed density

Figs. 8-10 display the ^{12}CO 2→1 line intensities, and the isotopic ^{12}CO/^{13}CO and ^{12}CO/C^{18}O 2→1 line ratios as functions of the FUV intensity χ and the cloud column density $\langle N\rangle$. In these models the hydrogen particle density was kept fixed at

$\langle n\rangle$=$4 \times 10^5 \mathrm{cm}^{-3}$. For $\langle N\rangle \gtrsim 10^{22}\mathrm{cm}^{-2}$ the line intensities and ratios are insensitive to χ. The ^{12}CO 2→1 line intensities increase for increasing cloud size. Stronger FUV fields result in somewhat weaker line intensities, especially for small clouds. The isotopic ratios are large when $\langle N\rangle$ and χ are large, and relatively small for large clumps and weak FUV fields. The line ratios are mainly affected by the different optical depths of the ^{12}CO, ^{13}CO and C^{18}O 2→1 lines. This difference implies that the spherical clouds are effectively smaller for the C^{18}O and ^{13}CO transitions than for the ^{12}CO transitions. Temperature gradient effects are less important.

4. Comparison with observations

Castets et al. (1990) and Kramer et al. (1996) have observed the ^{12}CO and ^{13}CO low-J lines in various star forming cloud complexes with χ in the range $100 \leq \chi \leq 1000$. Averaging the line intensities over different positions (c.f. Kramer et al.) the low-J line center brightness ratio is typically close to unity, both for the ^{12}CO and ^{13}CO lines. However, the ^{12}CO/^{13}CO ratio between the same transition is about 2-3, the ^{12}CO/C^{18}O ratio between the same transition is about 20. The absolute values of the line center brightness temperature is somewhat larger than 20 K for the ^{12}CO lines, about 10 K for the ^{13}CO lines and about 1-2 K for the C^{18}O lines. Castets et al. demonstrated that these ratios cannot be explained by single temperature, single density models. The spherical PDR models can reproduce the observations for densities of about $\langle n\rangle$=$4 \times 10^5 \mathrm{cm}^{-3}$ and column densities $\langle N\rangle \geq 10^{22}\mathrm{cm}^{-3}$. The model results are in this parameter range relatively insensitive to the intensity of the FUV field. At single positions the ^{12}CO/^{13}CO line ratio can vary between 1.5-8.0 (Kramer et al. 1996). This can again be explained by the spherical PDR models by varying the clump size and the densities. PDR models thus give a very natural explanation of the observed intensities.

5. Summary

In this paper we have presented model computations of low-J ^{12}CO/^{13}CO/C^{18}O emission from spherical clouds exposed to isotropic FUV radiation fields. The principal results of our investigations can be summarized as follows:

1. The ^{12}CO 2→1/1→0 line ratio is insensitive to the cloud gas density $\langle n\rangle$ and column density $\langle N\rangle$. This line ratio varies from values of 0.6 to 1.4 for low $\langle n\rangle$ large $\langle N\rangle$ clouds to high $\langle n\rangle$ small $\langle N\rangle$ clouds. The behavior of the ^{13}CO 2→1/1→0 line ratio is similar, with values ranging from 0.6 to 2.4.

2. Similarly, the ^{12}CO 3→2/2→1 line ratio ranges from 0.6 to 1.1, and the ^{13}CO 3→2/2→1 ratio ranges from 0.5 to 1.4.

3. The isotopic ratio of the ^{12}CO 2→1 and the ^{13}CO 2→1 line ranges from 1.8 for low $\langle n\rangle$ large $\langle N\rangle$ clouds to 7.0 for high $\langle n\rangle$ small $\langle N\rangle$ clouds. The ^{12}CO/^{12}C^{18}O 2→1 line ratio varies from 3 to > 100.

4. For a fixed FUV field strength $\chi = 1000$ the ^{12}CO 2→1 line center brightness temperature (averaged over the cloud surface) ranges from 1.1 K for a model with $\langle n\rangle = 10^4\mathrm{cm}^{-3}$ and $\langle N\rangle = 2.5 \times 10^{21}\mathrm{cm}^{-2}$ to 53 K for a model with $\langle n\rangle = 10^7\mathrm{cm}^{-3}$ and $\langle N\rangle = 4.0 \times 10^{22}\mathrm{cm}^{-2}$. The ^{13}CO 2→1 line intensities range from 0.5 K to 24 K. For small clouds C^{18}O is nearly fully photodissociated, and reaches a maximum value of ~ 4 K when $\langle n\rangle$ and $\langle N\rangle$ are large.

5. For clouds with $\langle N\rangle \geq 10^{22}\mathrm{cm}^{-2}$ the absolute and relative CO line intensities are insensitive to χ in the range 100 to 10^4.

6. Taken together, these statements show that the low-J ^{12}CO/^{13}CO line ratios in particular (but also the C^{18}O line ratios) are rather insensitive to the physical parameters of the UV-embedded clumps (density, column density, and UV-field strength). This implies on one hand, that the low-J isotopomeric CO line ratios are not useful diagnostics of these conditions. On the other hand, it is very satisfying that the models reproduce the narrow range of observed line ratios over a large range of realistic clump parameters. Thus, the scenario of clumpy molecular clouds, penetrated by UV-radiation through the diffuse interclump medium, provides a natural explanation for the narrow range of observed low-J CO line ratios, despite the large variation of physical paramters of those clumps within a molecular cloud.

Molecular cloud geometry is, of course, much more complex than spherical. The observed, fractal distribution of the observed line emission can, however, be modelled as a superposition of the emission from many clumps with a power law mass and size distribution over a large range in clump masses (Stutzki et al. 1998). Although superimposing the emission from many clumps will certainly change the resulting line ratios for the clump ensemble, condidering different beam filling factors and optical depth effects, it will keep the line ratios of the clump ensemble near the narrow range of line ratios found for the single clumps. The variation in the observed line ratios between different sources and regions within a source would then, in addition to systematic gradients e.g. in the average UV-field, result from the difference in the distribution of clumps along the particular sources or lines-of-sight: high total column density lines-of-sight will be dominated by a few, large and massive clumps, low column density lines-of-sight see mainly many small, unresolved clumps.

In a more detailed model clumps of different masses and sizes, embedded in a lower density interclump medium, will be illuminated by a UV field decreasing systematically from outside into the cloud. Such a model and its application to interpreting the emission distribution observed for particular sources will the topic of subsequent papers.

Acknowledgements. This research was supported by the Deutsche Forschungsgemeinschaft through Grant SFB 301. A. Sternberg thanks the Israel Science Foundation for Support.

References

Aalto S., Booth R.S., Black J.H., Johansson L.E.B., 1995, A&A 300, 369

Bakes E.L.O., Tielens A.G.G.M., 1994, ApJ 427, 822
Castets A., Duvert G., Dutrey A., et al., 1990, A&A 234, 469
Draine B.T., 1978, ApJS 36, 595
Gierens K.M., Stutzki J., Winnewisser G., 1992, A&A 259, 271
Heithausen A., Bensch F., Stutzki J., Falgarone E., Panis J.-F., 1998, A&A 331, L65
Hollenbach D.J., Takahashi T., Tielens A.G.G.M., 1991, ApJ 377, 192
Köster B., Störzer H., Stutzki J., Sternberg A., 1994, A&A 284, 545
Kramer C., Stutzki J., Winnewisser G., 1996, A&A 307, 915
Kramer C., Stutzki J., Röhrig R., Corneliussen U., 1998, A&A 329, 249
Langer W.D., Graedel T.E., Frerking M.A., Armentrout P.B., 1984, ApJ 277, 581
Le Bourlot J., Pineau des Forets G., Roueff E., FLower D.R., 1993, A&A 267, 233
Millar T.J., Farquhar P.R.A., Willacy K., 1997, A&AS 121, 139
Papadopoulos P.P., Seaquist E.R., 1998, ApJ 492, 521
Röhrig R., Stutzki J., Ungerechts H., Winnewisser G., 1995, In: The Physics and Chemistry of Interstellar Molecular Clouds. Springer, Berlin
Sakamoto S., Hayashi M., Hasegawa T., Handa T., Oka T., 1994, ApJ 425, 641
Schneider N., Stutzki J., Winnewisser G., Block D., 1998, A&A 335, 1049
Spaans M., Neufeld D., 1997, ApJ 484, 785
Sternberg A., Dalgarno A., 1995, ApJS 99, 565
Störzer H., Stutzki J., Sternberg A., 1996, A&A 310, 592
Stutzki J., Stacey G., Genzel R., et al., 1988, ApJ 332, 379
Stutzki J., Bensch F., Heithausen A., Ossenkopf V., Zielinsky M., 1998, A&A 336, 697
van der Werf P.P., Stutzki J., Sternberg A., Krabbe A., 1995, A&A 313, 633
van Dishoeck E.F., Black J.H., 1988, ApJ 334, 771
Wilson C.D., Howe J.E., Balogh M.L., 1999, ApJ 517, 174